DAMA and WIMP dark matter

Frank J. Petriello and Kathryn M. Zurek

Physics Department, University of Wisconsin,
Madison, WI 53706, U.S.A.
E-mail: `frankjp@physics.wisc.edu`, `kzurek@wisc.edu`

ABSTRACT: We study whether spin-independent scattering of weakly-interacting massive particles (WIMPs) with nuclei can account for the annual modulation signal reported by DAMA. We consider both elastic and inelastic scattering processes. We find that there is a region of WIMP parameter space which can simultaneously accommodate DAMA and the null results of CDMS, CRESST, and XENON. This region corresponds to an ordinary, elastically-scattering WIMP with a standard Maxwell-Boltzmann distribution, a mass $3 \text{ GeV} \lesssim m_{\text{DM}} \lesssim 8 \text{ GeV}$, and a spin-independent cross section with nucleons $3 \times 10^{-41} \text{ cm}^2 \lesssim \sigma_p^{\text{SI}} \lesssim 5 \times 10^{-39} \text{ cm}^2$. This new region of parameter space depends crucially on the effect of channeling on the energy threshold for WIMP detection in the DAMA experiment; without the inclusion of this effect, the DAMA allowed region is essentially closed by null experiments. Such low-mass WIMPs arise in many theories of Beyond the Standard Model physics, from minimal extensions of the MSSM to solutions of the baryon-dark matter coincidence problem. We find that inelastic scattering channels do not open up a significant parameter region consistent with all experimental results. Future experiments with low energy thresholds for detecting nuclear recoils, such as CDMSII-Si and those utilizing ultra-low energy germanium detectors, will be able to probe the DAMA region of parameter space.

KEYWORDS: Beyond Standard Model, Cosmology of Theories beyond the SM.

Contents

1. Introduction

Recently, the DAMA collaboration has provided further evidence for the observation of an annual modulation in the rates of nuclear recoil in their experiment [1]. Such a signal arises naturally from postulating Weakly Interacting Massive Particles (WIMPs) in the galactic halo that scatter from target nuclei in detectors. The annual modulation of the interaction rate comes from the variation in the relative velocity of the earth with respect to the galactic dark matter halo as the earth orbits the sun. This changes the flux of dark matter particles and the size of their interaction cross-sections, with expected extrema occurring at June 2 and December 2. The DAMA experiment observes a maximum at low nuclear recoil energies on May 24, plus or minus 8 days, and they have accumulated enough data to put the significance of the observed modulation at approximately 8σ. Both the phase and amplitude of the signal are highly suggestive of WIMP interactions. The collaboration has not been able to identify other systematic effects capable of producing this signal, and have claimed that the annual modulation is a discovery of dark matter. This claim has been controversial, partly because a number of other experiments seem to be in direct contradiction. In particular, the original DAMA allowed region with WIMP mass $30 \text{ GeV} \lesssim m_{\text{DM}} \lesssim 200 \text{ GeV}$ and dark matter-nucleon interaction cross-section $\sigma_p \simeq 10^{-41} - 10^{-42} \text{ cm}^2$ had been quite conclusively ruled out by the CDMS [2–4] and XENON [5] experiments for the case of an elastically scattering WIMP.

Methods of reconciling the DAMA signal with the results of other experiments have been proposed in the past. Inelastic scattering processes, $\chi_1 N \to \chi_2 N$, where χ_1 is the dark matter particle and χ_2 is another new state with mass splitting δ between the states,

have been proposed in the context of supersymmetric models [6–8]. Inelastic scattering of MeV dark matter particles to lighter states was investigated as a possible solution in ref. [9]. Mirror states from a hidden-sector copy of the Standard Model have been proposed as a candidate consistent with all experimental constraints [10, 11], as have various models with heavy composite states [12]. A model-independent study of spin-independent elastic scattering noted that scattering from the sodium component of the NaI DAMA scintillators allowed a small window of dark matter masses in the $5 - 9\,\mathrm{GeV}$ to be consistent with current experimental constraints [13, 14]. This study noted that since sodium nuclei are lighter than germanium nuclei, the threshold for scattering off sodium could be lower than that for germanium for light dark matter states. It was also shown previously that spin-dependent scattering may open up additional parameter space consistent with DAMA and other experiments [15].

This model-independent study of elastic scattering in ref. [14] is no longer applicable, as several new results have appeared recently. New experimental constraints and improved understanding of scattering processes in the DAMA apparatus have drastically altered both the excluded parameter space and the physics underlying the DAMA modulation signal. We perform a model-independent study of both elastic and inelastic scattering mechanisms accounting for all recent experimental measurements. We find that completely ordinary, spin-independent elastically scattering WIMPs with masses in the range $3 - 8\,\mathrm{GeV}$ and scattering cross sections in the range $3 \times 10^{-41}\,\mathrm{cm}^2$ to $5 \times 10^{-39}\,\mathrm{cm}^2$ are consistent with all experimental constraints. No additional dark matter stream is needed; a simple Maxwell-Boltzmann distribution allows this parameter space. Inelastic scattering no longer opens up a significant region of additional allowed parameter space. We summarize here the important features and conclusions of our analysis.

- We include the effect of channeling in the NaI crystal scintillators of DAMA, an effect recently noted in ref. [16] and studied by the DAMA collaboration [17]. Channeling occurs in crystalline detectors where the only signal measured is the light output, and when recoiling nuclei transfer energy only to the electrons of the detector material because of either their direction of motion or incident energy. The effect of channeling is to remove the quenching factor usually required to convert between nuclear recoil energy and electron-equivalent energy, and in the context of dark matter searches it effectively lowers the energy threshold for detection of nuclear recoils of DAMA below that of CDMS and XENON. This effect is crucial in reconciling elastically scattered WIMPs consistent with all experimental constraints. In particular, the lower threshold of DAMA means that it can detect lighter dark matter particles than the higher threshold experiments like CDMS and XENON. This effect opens the region of light WIMP parameter space for DAMA. We note that the presence of channeling in the energy regime studied by DAMA has not been conclusively established, although it has been observed in NaI crystals at higher energies [18].

- We include constraints from CDMS-SUF, CDMS-II, CRESST-I scattering from sapphire targets [20], and XENON. Inclusion of experimental results from multiple target

nuclei is necessary to correctly elucidate the allowed parameter region. In the elastic scattering case we also include the recent results from the CoGeNT collaboration [19].

- We study spin-independent elastic scattering, and inelastic scattering with either positive or negative mass splitting δ between the incident and scattered dark matter particle. Inelastic scattering of either sign opens up only a very small window of parameter space; roughly, inelastic scattering to heavy states is ruled out by XENON and the germanium data from CDMS-II, while scattering to lighter states is ruled out by CRESST and the silicon data from CDMS. The preferred parameter space is for light mass dark matter with elastic scattering. Future results from ultra-low noise germanium detectors [21] [1], and the lower threshold silicon data from CDMS will be vital in exploring this region. The low threshold germanium experiment TEX-ONO [22] may also be able to probe this region, though its sensitivity has recently been called into question [23] (inclusion of current TEXONO constraints does not change our results).

There are many possible models which could give rise to such a comparatively light WIMP. In extensions of the Minimal Supersymmetric Model, for example, GeV mass WIMPs with the right relic abundance arise [24, 25]. It has been shown that hidden sectors in the context of supersymmetric models give rise naturally to WIMPs with GeV or even lighter masses, as observed in refs. [26, 27]. It was shown explicitly that the models of this sort can account for the DAMA signal [28]. Supersymmetric models with non-unified gaugino masses at the grand unified scale give rise to light neutralino dark matter candidates [29]; the importance of the channeling effect for these models was noted in ref. [30], as was the effect of having the light sodium component of the DAMA target. Lastly, solutions to the baryon-dark matter asymmetry problem also predict a WIMP with a mass in the range, $m_{dm} \approx \Omega_{dm}/\Omega_b m_p \approx 5m_p$ [31 − 34]. It is clear that the light dark matter paradigm suggested by the direct detection experiments raises numerous theoretical questions and has phenomenological impact on a broad array of experiments. We leave the potential implications of light WIMPs to future work, and focus here on clarifying the experimental situation.

The outline of the paper is as follows. In section 2 we review the formalism of direct detection of dark matter. We review the characteristics of the relevant experiments, discuss the physics and implications of the channeling effect in DAMA, and discuss our analysis method. We then apply these techniques to derive the allowed parameter space consistent with all experimental measurements for both elastically and inelastically scattered WIMPs in section 3. Finally, we conclude and discuss future directions.

2. Rates for direct detection of dark matter

2.1 Direct detection formalism

We first review the relevant features of direct detection of dark matter by WIMP-nucleus

---

[1]We thank J. Collar for correspondence regarding the ability of these experiments to probe this region.

scattering. The differential rate per unit detector mass in nuclear recoil energy is given by

$$\frac{dR}{dE_R} = N_T \frac{\rho_{\text{DM}}}{m_{\text{DM}}} \int_{|\vec{v}|>v_{\min}} d^3v \, v f(\vec{v}, \vec{v_e}) \frac{d\sigma}{dE_R}. \tag{2.1}$$

Here, N_T is the number of target nuclei per unit mass, m_{DM} is the dark matter particle mass, and $\rho_{\text{DM}} = .3\,\text{GeV/cm}^3$ is the local dark matter halo density. $\vec{v}$ is the dark matter velocity in the frame of the Earth, $\vec{v_e}$ is the velocity of the Earth with resepect to the galactic halo, and $f(\vec{v}, \vec{v_e})$ is the distribution function of dark matter particle velocities. We take $f(\vec{v}, \vec{v_e})$ to be a standard Maxwell-Boltzmann distribution:

$$f(\vec{v}, \vec{v_e}) = \frac{1}{(\pi v_0^2)^{3/2}} e^{-(\vec{v}+\vec{v_e})^2/v_0^2}. \tag{2.2}$$

The Earth's speed relative to the galactic halo is $v_e = v_\odot + v_{\text{orb}} \cos\gamma \cos[\omega(t-t_0)]$ with $v_\odot = v_0 + 12\,\text{km/s}$, $v_{\text{orb}} = 30\text{km/s}$, $\cos\gamma = 0.51$, $t_0 = \text{June 2nd}$, and $\omega = 2\pi/\text{year}$. We set the most probable dark matter speed in the galactic frame to $v_0 = 220\,\text{km/s}$ for most of our analysis, but study the effect of allowing it to vary within its 90% C.L. range $170\,\text{km/s} \leq v_0 \leq 270\,\text{km/s}$ [35]. The upper limit of the velocity integration of eq. (2.1) should be taken as the galactic escape velocity, $490\,\text{km/s} \leq v_{\text{esc}} \leq 730\,\text{km/s}$ at 90% C.L. [35]. For simplicity we take the upper limit to infinity and *a postieri* restrict the minimum velocity to lie above v_{esc}. We set $v_{\text{esc}} = 730\,\text{km/s}$ for our study, but again study the effect of varying it within the 90% C.L. range. Neither uncertainty has a significant effect on our conclusions. The minimum dark matter velocity $v_{\min}$ depends on the recoil energy E_R and the details of the direct detection process, and will be discussed later.

We assume a spin-independent cross section between dark matter particles and nuclei; a standard calculation [36] leads to

$$\frac{d\sigma}{dE_R} = \frac{m_N}{2v^2} \frac{\sigma_p}{\mu_n^2} \frac{[f_p Z + f_n(A-Z)]^2}{f_n^2} F^2(E_R). \tag{2.3}$$

μ_n is the reduced mass of the dark matter particle and nucleon (proton or neutron), σ_p is the scattering cross section of the dark matter particle with nucleons, and $f_{n,p}$ are the coupling strengths of the dark matter particle to neutrons and protons respectively. $f_{n,p}$ are calculated from a coherent sum over the couplings to the quark model constituents of the nucleon. Z and A are the proton and atomic numbers of the nucleus, while $F(E_R)$ is a nuclear form factor which corrects for the above formula being strictly correct only as the momentum transfer $q^2 = 2m_N E_R \to 0$. We use a standard Helm form factor [37].

Inserting the dark matter-nucleus scattering cross section of eq. (2.3) into the differential rate in eq. (2.1) and performing the integration, we obtain the differential rate

$$\frac{dR}{dE_R} = \frac{N_T m_N \rho_{\text{DM}}}{4v_0 m_{\text{DM}}} \frac{\sigma_p}{\mu_n^2} \frac{[f_p Z + f_n(A-Z)^2]}{f_n^2} F^2(E_R) \left\{ \frac{\text{erf}(x_{\min}+\eta) - \text{erf}(x_{\min}-\eta)}{\eta} \right\}$$
$$\times \Theta(v_{\text{esc}} - v_{\min}(E_R)). \tag{2.4}$$

We have introduced the parameters $x_{\min} = v_{\min}/v_0$ and $\eta = v_e/v_0$. The Θ function accounts for our treatment of the maximum allowed dark matter velocity, as discussed above. We

will use the formula in eq. (2.4) to interpret the results of various direct detection searches for dark matter particles. We follow the standard convention and set $f_p = f_n$; results for other exchange mechanisms, such as Z-boson exchange, can be derived by scaling the cross section σ_p appropriately. The total number of nuclear recoil events in a recoil energy range between E_r^1 and E_r^2 is

$$N = \sum_i \int_{E_r^1}^{E_r^2} \frac{dR_i}{dE_r} \frac{\mathcal{E}_i}{N_T M_i} dE_r \tag{2.5}$$

where the sum is over each nuclear species i in the detector. $\mathcal{E}_i$ is the effective exposure of species i expressed in kg-days. We can parametrize $\mathcal{E}_i = M_i t \epsilon$, where t is the time of exposure, M_i is the target mass of species i, and ϵ is a detection efficiency.

2.2 Experimental constraints

We discuss the direct detection signal obtained by DAMA and the constraints imposed by other null experiments. The DAMA collaboration has recently reported an 8.2σ signal for an annual modulation signature of dark matter scattering [1]. This signal has been reported for several years, and the significance of the effect has been constantly increasing. It is convenient to parametrize the DAMA detection rate as

$$R_i = R_i^0 + S_i^1 \cos[\omega(t - t_0)], \tag{2.6}$$

where $t_0 = \text{June 2nd} = 152.5$ days is the time when the Earth is moving with its maximum speed with respect to the galactic halo and $T = 2\pi/\omega = 1\,yr$. The subscript i denotes different energy bins. The values measured by the collaboration in the $2 - 6\,\text{keVee}$ bin are $t_0 = 144 \pm 8$ days and $T = 0.998 \pm 0.003$ yr. The keVee unit is keV-electron-equivalent, which accounts for quenching of unchanneled events; we describe this effect in detail in the next subsection. For the moment, we only comment that keVee = keV for channeled events, and keVee = q keV, where $q < 1$, for unchanneled events. The constant term R_i^0 is composed of both a signal piece coming from dark matter initiated processes, and a background piece arising from other sources of nuclear recoil: $R_i^0 = b_i^0 + S_i^0$. The expressions for S_i^0 and S_i^1 are obtained by integrating eq. (2.4) over a given range of E_R. More precisely, expanding the interaction rate in a Taylor series around $v_e = v_\odot$ for an energy interval between E_i and $E_i + \Delta E_i$, we have

$$R_i^0 = \frac{1}{\Delta E} \int_{E_i}^{E_i + \Delta E_i} \left(\frac{dR}{dE_r} \right) dE_r \tag{2.7}$$

and

$$R_i^1 = \frac{\Delta v_e}{\Delta E} \int_{E_i}^{E_i + \Delta E_i} \frac{\partial}{\partial v_e} \left(\frac{dR}{dE_r} \right) dE_r, \tag{2.8}$$

where the differential rates are to be evaluated at $v_e = v_\odot$ and $\Delta v_e = v_{\text{orb}} \cos \gamma$.

The DAMA collaboration has not been able to find another effect besides dark matter scattering that could contribute to S_i^1. The modulation amplitudes reported by DAMA in each energy bin are given in table 1. Non-zero modulation is clearly observed in the low energy bins, while it is absent in the $6 - 14$ keVee bin.

Energy	S_i^1 (cpd/kg/keVee)
$2-4$ keVee	0.0223 ± 0.0027
$2-5$ keVee	0.0178 ± 0.0020
$2-6$ keVee	0.0131 ± 0.0016
$6-14$ keVee	0.0009 ± 0.0011

Table 1: Modulation amplitudes in units of counts-per-day/kilograms/keVee as reported by DAMA [1]

Experiment	Target	Exposure (kg-d)	Threshold	Ref
CDMS-SUF	Ge	65.8	5 keV	[2]
	Si	6.58	5 keV	
CDMS-II	Ge	121.3	10 keV	[3]
	Si	12.1	7 keV	[4]
XENON10	Xe	131	4.5 keV	[5]
CRESST-I	Al_2O_3	1.51	0.6 keV	[20]

Table 2: Relevant features of the null experiments used in our analysis.

Any dark matter model allowed by the DAMA results must be consistent with other null experiments. We consider constraints imposed by the CDMS, CRESST, and XENON collaborations. We summarize the salient features of each experiment, including the target nucleus, energy threshold, and exposure, in table 2. Considering the constraints from a variety of experiments is vital, as each is relevant for different regions of dark matter parameter space. We will see this explicitly in our numerical results of section 3. The most important qualitative observation to make about the experiments is the difference in the energy thresholds. The recoil energy is related to the mass of the incoming dark matter particle through the relation

$$E_R = \frac{2v^2 \mu_{\text{nuc}}^2}{m_N}, \tag{2.9}$$

where μ_{nuc} the reduced mass of the WIMP-*nucleus* system and v their relative velocity. It follows that for low mass WIMPs, the recoil energy of the nucleus is not high enough to be above threshold for XENON and CDMS, while it is for DAMA. The experiments which do have thresholds competitive with DAMA, in particular the CRESST-I experiment, have much lower exposures. While they constrain the low dark matter mass region, their limits on the cross-section σ_p are not strong enough to constrain much of the DAMA parameter space. We show in section 3 that the CDMS-II Si run is also sensitive to lower dark mater masses because of the lower target mass of silicon and the lower threshold compared to the germanium data.

2.3 The physics of quenching and the DAMA signal

Since it has important implications for dark matter searches, we discuss in more detail the physics of the channeling and quenching effects which allow the compatibility of the DAMA

signal with other null experiments. The relevance of this effect for the current analysis is that DAMA is sensitive to nuclear recoil energies down to 2 keV, below the threshold of both XENON and CDMS.

The light yield of scintillators is different depending on whether the incident particles interact electromagnetically or via the nuclear force. The bookkeeping for this is performed by introducing an electron equivalent recoil energy for a given nuclear recoil energy; for a nuclear recoil of 1 keV, the equivalent electron energy (in keVee) is $q_x \times 1\,\text{keV}$. q_x is the quenching factor for the nuclear material composing the scintillator; for the materials composing the DAMA detectors, $q_{Na} \approx 0.3$ and $q_I \approx 0.09$. It is simple to understand why $q < 1$ and the electron equivalent energy is less than that of the nuclear recoil energy. A nucleus hitting scintillator material will lose energy both by electromagnetic and nuclear interactions, while an incoming electron will lose energy only via electromagnetic interactions. It is primarily the production of radiation in electromagnetic interactions that produces the light yield in the scintillating material, yielding $q < 1$.

For crystal scintillators such as those used by DAMA, a portion of the events will be "channeled," effectively changing the quenching factor to $q \approx 1$. This occurs when incident particles transfer energy only to the electrons of the scintillator material. This can occur for certain energies and incidence angles of the incoming particle. The importance of this for the DAMA experiment was first discussed in ref. [16], and a detailed analysis of its effect was performed by the DAMA collaboration in ref. [17]; we refer the reader to these references for a more detailed discussion. An estimate of the fraction of channeled events based on simulation is given in figure 4 of ref. [17]. We use the following simple parametrization in our analysis [11]:

$$f_{Na} \simeq \frac{1}{1 + 1.14 E_R(\text{keV})}, \ f_I \simeq \frac{1}{1 + 0.75 E_R(\text{keV})}. \tag{2.10}$$

The other experiments considered in our study do not report this distinction between quenched and channeled events. CDMS collects all recoil energy from ionization and phonons (heat). Channeling does not occur in liquid noble gases [17], such as used in XENON. CRESST sets $q = 1$ in their analysis. The XENON collaboration has incorporated the appropriate quenching factor into their published results.

2.4 Analysis procedure

We now discuss our analysis procedure for determining whether the DAMA results are consistent with the constraints of other experiments for both elastic and inelastic dark matter scattering. For experiments that report no events above background, we demand that dark matter initiated scattering produce less than 2.3 events throughout the entire range analyzed, as appropriate for establishing a 90% C.L. upper limit. For experiments that report events but ascribe them to background processes, we adopt a conservative approach and include the events when setting limits. We determine the 90% C.L. limit on the dark matter cross section in the presence of this background using a simplified version of the optimum interval method [38]. We divide the data into energy bins using the published results. We study all contiguous combinations of bins, and demand that the

dark matter candidate produce no more than the 90% C.L. upper limit allowed events as dictated by Poisson statistics in each such interval. The most stringent limit in σ_p for a given $m_{\rm DM}$ among the studied intervals is then used. This procedure allows effective use of the different kinematics of each dark matter particle when setting constraints, as the appropriate energy bins which constrain a given dark matter candidate depend strongly on the mass and whether elastic or inelastic scattering is considered. Our technique reproduces reasonably well the published constraints in the elastic scattering limit, as obtained from either the experimental papers or DMTools [39].

For completeness, we now describe in detail our treatment of each experimental data set.

- **DAMA**: For the DAMA signal, we perform a χ^2 fit to the $2-6$ and $6-14$ keVee bins given in table 1 for a given $m_{\rm DM}$ and σ_p:

$$\chi^2 = \sum_i \left(\frac{R_i^1 - R_i^{1,exp}}{\sigma_i} \right)^2 , \tag{2.11}$$

where $R_i^{1,exp}$ is the value of R_i^1 measured by DAMA in the ith energy bin, R_i^1 is the rate computed at a given $(m_{\rm DM}, \sigma_p)$ point, and σ_i is the experimental error on $R_i^{1,exp}$. The minimum χ^2 is found at a given $m_{\rm DM}$ by scanning over σ_p. Once the minimum χ^2 is found, if $\chi^2_{\rm min} < 2$, a 90% C.L. region is determined by accepting values of σ_p with $\chi^2 - \chi^2_{\rm min} < 2.71$. We also determine a 3σ allowed range for σ_p by accepting cross sections leading to $\chi^2 - \chi^2_{\rm min} < 9$.

- **CDMS-II**: The latest results from the five-tower germanium run of CDMS indicate no events in a nuclear recoil energy range of $10-100\,{\rm keV}$ [3]. The efficiency is fairly flat, and it has already been included in the effective exposure given in table 2. We demand that a dark matter candidate produce < 2.3 events to establish a 90% C.L. upper limit on σ_p for a given $m_{\rm DM}$. We also include the constraint from the silicon run of ref. [4]. The energy window for this result is $7-100\,{\rm keV}$; the lighter mass of silicon and the lower energy threshold leads to important constraints for light dark matter. We again demand that dark matter interactions produce < 2.3 events.

- **CDMS-SUF**: We include constraints from the CDMS run reported in ref. [2]. This early run has implications for light dark matter because the analysis threshold was set at 5 keV. The efficiency is not flat as a function of energy. We use the parametrized form given in ref. [14]:

$$\epsilon = \begin{cases} 7.6\% & E < 10\,{\rm keV} \\ 22.8\% & 10\,{\rm keV} < E < 20\,{\rm keV} \\ 38\% & E > 20\,{\rm keV}. \end{cases} \tag{2.12}$$

This function must be included in the integration of eq. (2.5). The experiment does observe events in the expected dark matter signal range, although these are consistent with background expectations. We determine the 90% C.L. limit on the dark matter

scattering rate in the presence of this background using a simplified version of the optimum interval method discussed above. We divide the data into the four energy bins $E < 10\,\text{keV}$, $10\,\text{keV} < E < 20\,\text{keV}$, $20\,\text{keV} < E < 55\,\text{keV}$, and $E > 55\,\text{keV}$. We obtain the background events in each bin from ref. [2].

- **XENON**: We include the first results from the XENON dark matter search reported in ref. [5]. We again apply the optimum interval method using the efficiencies and energy bins given there, and the reported background events. All observed events are attributed to background processes by the collaboration, but we follow their analysis in including the observed events when computing a limit.

- **CRESST**: The initial run of the CRESST experiment utilized a sapphire target with a low threshold of 0.6 keV [20]. We use the observed spectrum without background subtraction given in that reference. The collaboration attributes all observed events to background initiated processes, due to a study of coincident counts in multiple detectors. We apply the optimum interval method with a restriction that the interval size be greater than 1.2 keV, which is twice the experimental energy resolution. We use a 100% efficiency for detection of events, as reported by the collaboration.

- **TEXONO**: The TEXONO collaboration has recently reported results using a germanium target with a 200 eVee nuclear recoil energy threshold [22]. The limits claimed in this paper (but questioned in [23]) do not yield significant improvement over CRESST-I. We have checked that the $3-8\,\text{GeV}$ WIMP mass window is still open with or without the inclusion of TEXONO constraints in the current analysis. Their projected sensitivity, however, cuts deeply into the DAMA parameter space. We include the future projections in our analysis.

- **CoGeNT**: In the elastic scattering case we include the recent result of the CoGeNT collaboration [19]. The current exclusion curve reported by the collaboration does not include the possible effect of channeling. It is currently unclear by how much Ge-based ionization detectors such as used in CoGeNT are affected by channeling. We caution the reader that the CoGeNT exclusion curves could drift on our plots when channeling in this type of detector is simulated. Without channeling factored in, the measurement does not close the light WIMP window opened up by the channeling effect in the DAMA experiment, although future results from the collaboration should either confirm or severely constrain the DAMA parameter region.

3. Implications for models of WIMP dark matter

Following the analysis procedure described in the previous section, we study whether parameter space exists in which spin-independent dark matter scattering off nuclei can simultaneously accommodate the DAMA modulation signal and satisfy the constraints from other experiments. We begin by considering the case of elastic scattering. We then examine whether inelastic scattering processes of the form $\chi_1 N \to \chi_2 N$, where χ_2 can be

either lighter or heavier than the dark matter particle χ_1, can account for all experimental observations.

3.1 Elastic scattering

We present in figure 1 the results of our parameter space scan for spin-independent dark matter scattering. The inner and outer hatched regions respectively denote the 90% C.L. and 3σ regions consistent with the DAMA modulation signal. Regions above each colored line are excluded by the indicated experiments. Although a portion of the region consistent with DAMA is excluded, a region with $m_{\mathrm{DM}} \sim 3 - 8\,\mathrm{GeV}$ is not excluded. Two features of current experiments make this possible. Substituting the 4.5 keV threshold for XENON and the 10 keV threshold for CDMS-II into eq. (2.9) and setting $v = v_{\mathrm{esc}} = 730\,\mathrm{km/s}$, we see that XENON can only probe $m_{\mathrm{DM}} > 7\,\mathrm{GeV}$, while CDMS-II germanium is sensitive to $m_{\mathrm{DM}} > 8\,\mathrm{GeV}$. Although these experiments have large exposures, the light dark matter region is inaccessible to them. Further running of these experiments will not completely remove this window. The experiments with low enough thresholds to be sensitive to the DAMA region, notably CRESST, the 7 keV CDMS-II silicon run, and CoGeNT, do not have a large enough exposure, as seen from table 2.

Several distinct structures are noticeable in the DAMA allowed region. The low mass tail extending to large cross sections arises from channeled sodium events. Both the low threshold and light nucleus cause these to appear first as m_{DM} is increased. The allowed region above $m_{\mathrm{DM}} \approx 50\,\mathrm{GeV}$ arises from quenched iodine events. The presence of channeling is crucial for reconciling the DAMA signal with other null experiments. This is illustrated in figure 2, where the effects of channeling have been removed. No region in parameter space is consistent with all experiments when channeling is not considered.

The previous analysis of elastic scattering in ref. [14] utilized the light mass of sodium to render DAMA consistent with other experiments. At the time, all events in DAMA were considered to be quenched, leading to an approximately $2\,\mathrm{keV}/q_I \approx 7\,\mathrm{keV}$ energy threshold for scattering off sodium. Although this threshold is similar to the thresholds of other experiments, sodium is lighter than other nuclei such as germanium, so that the net effect is sensitivity to lighter dark matter particles. This led to the low-mass tail in figure 2. New limits from the 7 keV silicon run of CDMS-II have completely ruled out this region, although as shown in ref. [14] it is possible that fitting to the $2 - 4$ keV bin instead of the $2 - 6$ keV bin might open up a small amount of additional parameter space. The channeling effect is required to open a significant low-mass elastic scattering window.

To roughly study the effect of galactic uncertainties on these results, we also show in figure 3 the effect of changing the most-probable speed v_0 and the galactic escape velocity. In the left panel we change to $v_0 = 170\,\mathrm{km/s}$, while in the right panel we set $v_{\mathrm{esc}} = 610\,\mathrm{km/s}$. Although both changes have quantitative effects, the picture described above is unchanged. Previous analyses have shown that assuming a galactic velocity distribution beyond a simple Maxwell-Boltzmann form opens up a small region of additional allowed parameter space [14], and we expect the same would occur in our study, though we do not pursue it further here.
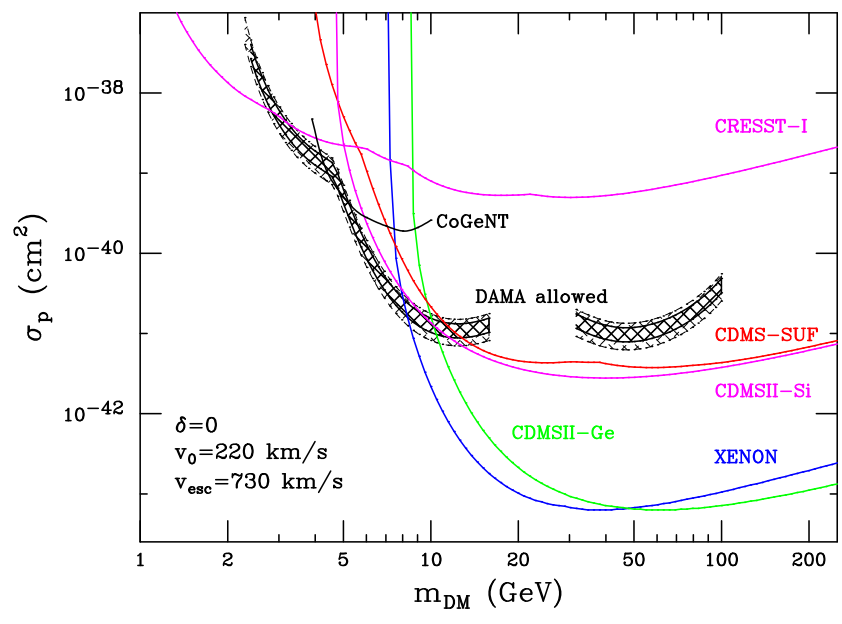
Figure 1: Allowed region in the m_{DM}, σ_p plane consistent with the DAMA modulation signal at 90% C.L. and 3σ (inner and outer hatched regions, respectively). Also shown are the experimental constraints arising from other null experiments. The DAMA allowed region includes both channeled and quenched events.
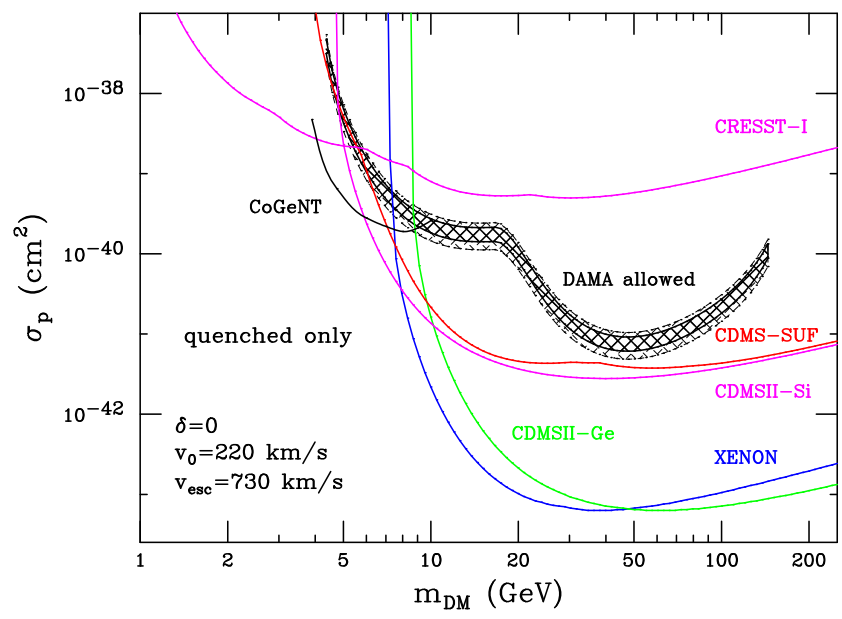

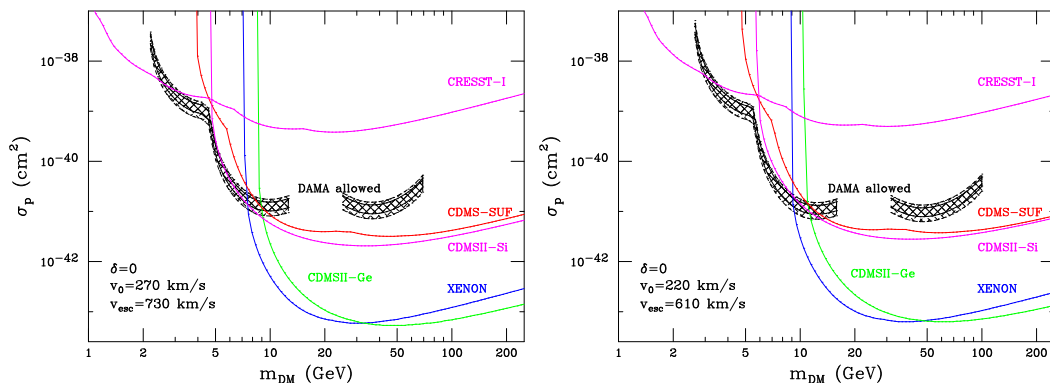**Figure 2:** Similar to figure 1, but if DAMA observed only quenched events. The presence of un-quenched (channeled) events is necessary to reconcile DAMA with null experiments.

Figure 3: Region allowed by the DAMA modulation signal together with other experimental constriants obtained by changing to $v_0 = 270\,\mathrm{k/s}$ (left panel) and $v_{esc} = 610\,\mathrm{km/s}$ (right panel).

Further running of these experiments will continue to probe the elastic scattering parameter space. To estimate whether future experiments can rule out the allowed region, we show in figure 4 the projected sensitivities of XENON, CDMSII-Si, and TEXONO together with the DAMA allowed region. These projections are obtained by simple scalings of the current exposure by a factor of ten. For CDMS-II, the expected signal has been increased by ten, while for XENON the expected signal and observed background have both been scaled upward. While the XENON energy threshold is currently too high to probe the DAMA allowed region, future CDMSII silicon data will test dark matter in the $5-8\,\mathrm{GeV}$ range. For TEXONO, we have assumed an exposure of 1 kg-yr, the future goal of the collaboration [22]. For CoGeNT, we have used the projected bound from ref. [19] expected after an ongoing detector upgrade. Achievement of these goals will allow both CoGeNT and TEXONO to study the entire low-mass WIMP window.

In summary, completely ordinary, elastically scattering WIMPs with masses in the $3-8\,\mathrm{GeV}$ range can produce the DAMA modulation signature and remain consistent with other experimental constraints. Future data, particularly those from the silicon detectors of CDMSII, from TEXONO and from other low-threshold Germanium experiments such as used by the CoGeNT collaboration, are critically important to probe this parameter region.

3.2 Inelastic scattering

Inelastic scattering has also been considered as a mechanism for explaining the DAMA signal. In models of this type, scattering processes $\chi_1 N \rightarrow \chi_2 N$ are considered. N denotes the target nucleus and χ_1 is the dark matter candidate. The final-state particle χ_2 can have a different mass than χ_1. We denote the mass splitting by $\delta \equiv m_2 - m_1$. δ is positive for heavier final states, such as in the supersymmetric model of refs. [7, 8]. Negative δ has been studied as a possible phenomenological explanation of the DAMA signal in ref. [9].

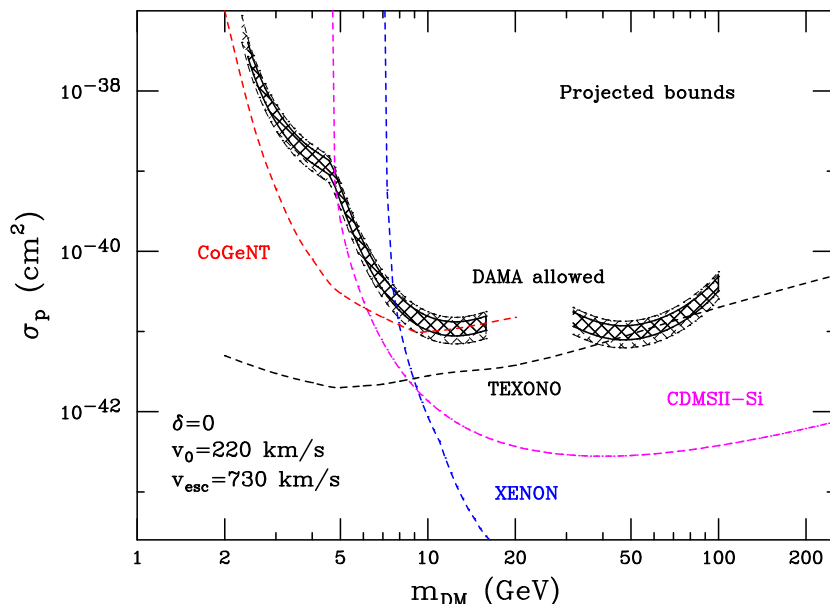In the case of inelastic scattering, the maximum recoil energy can be shown by kine-

Figure 4: Projected sensitivities of XENON and CDMSII-Si obtained by scaling the current exposures upwards by a factor of ten. For XENON, both signal and observed background are scaled upwards, For TEXONO, the projected sensitivity has been read off from [22], while for CoGeNT the projected sensitivity is taken from [19].

matics to be

$$E_R^{\max} = \frac{\mu_1}{m_N} \left\{ \mu_1 \beta^2 - \delta + \sqrt{\mu_1^2 \beta^4 - 2\mu_1 \delta \beta^2} \right\} . \tag{3.1}$$

Equivalently, for a given recoil energy, the dark matter must have a minimum velocity $v_{\min}$ to scatter off a nucleus which is

$$v_{\min} = \sqrt{\frac{1}{2m_N E_R}} \left(\frac{m_N E_R}{\mu_1} + \delta \right) . \tag{3.2}$$

Here, $\mu_1 = m_1 m_N / (m_1 + m_N)$ is the reduced mass of the nucleus and χ_1, and β is the velocity of χ_1 in units of c. Inelastic dark matter with $\delta > 0$ reconciled DAMA with the null experiments through two main effects [7, 8]. First, for a sufficiently large mass splitting, only heavier targets can scatter inelastically for an experiment with a threshold E_R^{th}. The restriction present in eq. (3.1) that the dark matter velocity $\beta^2 > 2\delta/\mu_1$ becomes increasingly stringent as μ_1 is decreased. Since iodine is relatively heavy in comparison to germanium, this could enhance the signal in DAMA relative to the germanium of CDMS. This argument becomes much less effective with the presence of XENON constraints, since the mass of xenon is similar to iodine. Second, positive δ changes the shape of the recoil energy spectrum, suppressing low energy recoils with respect to high energy ones. Since before the discovery of channeling it was thought that the thresholds of DAMA were higher than those of the null experiments, DAMA favored inelastic dark matter.

However, we find that with the inclusion of channeled events and the new constraints from XENON and CDMS-II, inelastic dark matter becomes severely constrained. We
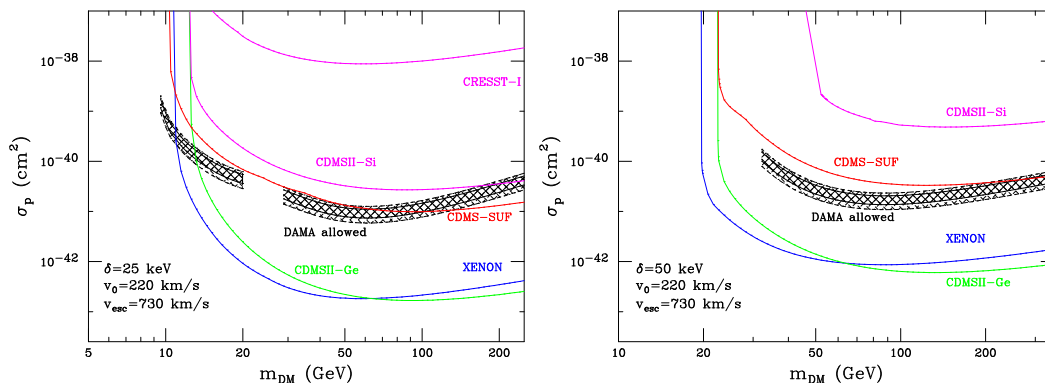
Figure 5: Region allowed by the DAMA modulation signal together with other experimental constraints in the m_{DM}, σ_p plane for $\delta = 25, 50 \, \text{keV}$.

show in figure 5 the DAMA allowed parameter space together with other experimental constraints for the representative values $\delta = 25, 50 \, \text{keV}$. The region of weak scale dark matter $m_{DM} \sim 100$ GeV and 100 keV mass splittings proposed in [7, 8] is closed. The new experimental constraints from XENON and the germanium run of CDMS-II are too severe. The small sliver of allowed parameter space present in the $\delta = 25 \, \text{keV}$ case arises from channeled scatterings from iodine. Although some regions for not-too-large δ are still consistent with all measurements, inelastic scattering with $\delta > 0$ does not open up significant parameter space beyond elastic scattering.

There are two additional features to note in figure 5. First, relative to the $\delta = 0$ case, positive δ shifts the region allowed by DAMA to larger masses. This occurs because of the higher incident energy required to push the scattering over threshold. Second, the constraints from experiments with light targets such as CRESST become much less significant. The constraint on the initial dark matter velocity $\beta^2 > 2\delta/\mu_1$ discussed before indicates that for light nuclei, only the high velocity tail of the Maxwell-Boltzmann distribution can lead to dark matter scattering.

We now study the region $\delta < 0$. We display in figure 6 the DAMA allowed parameter space together with other experimental constraints for the representative values $\delta = -25, -50 \, \text{keV}$. The DAMA allowed region shifts to lower dark matter masses. The lighter-mass horseshoe-shaped region is associated with channeled events from sodium, while the region for slightly higher masses comes from both quenched sodium and channeled iodine events. The lack of an allowed region at masses higher than roughly 10 GeV occurs because the phase of the DAMA signal cannot be correctly obtained; a minimum in the dark matter scattering rate is predicted at $t_0 = $ June 2nd rather than a maximum. Only a small sliver of the higher-mass region is consistent with all measurements, with the light-mass parameter space arising from sodium events ruled out by CRESST. The increasing severity of the these constraints as δ is descreased can be understood by studying the regions of the Maxwell-Boltzmann distribution contributing to dark matter scattering as a function of δ. Only a small portion of the Maxwell-Boltzmann distribution can initiate
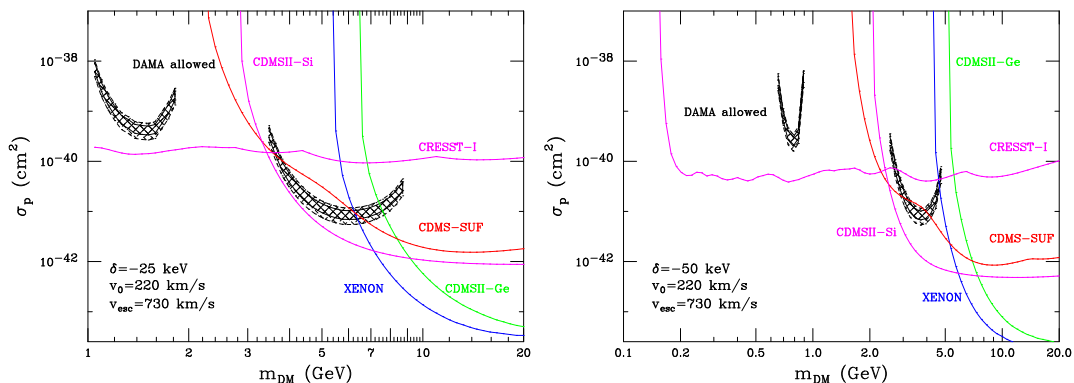
Figure 6: Region allowed by the DAMA modulation signal together with other experimental constraints in the $m_{\mathrm{DM}}, \sigma_p$ plane for $\delta = -25, -50 \,\mathrm{keV}$.

scattering for $\delta \geq 0$. Lower velocities very quickly begin to lead to scattering as δ is decreased, strengthening the constraints for negative δ. The sharp turn-off of the CRESST constraints at low dark matter masses visible in figure 6 follows from the fact that eq. (3.1) requires that $m_1 \gtrsim m_N E_R^{\mathrm{thresh}} / (\sqrt{2 m_N E_R^{\mathrm{thresh}} \beta_{\mathrm{esc}}^2} + |\delta|)$ for dark mater particles significantly lighter than the target nucleus. We note that the wiggles visible in the exclusion curves arise from our use of the binned optimum interval method; as the kinematics of the dark matter scattering changes, a different energy interval is selected to provide the most stringent constraint.

Finally, we show in figure 7 the region in the m_{DM}, δ plane consistent with both the DAMA signal and all considered experimental constraints. Dark matter masses in the region $3 - 13\,\mathrm{GeV}$ and mass splittings in the range $-15\,\mathrm{keV} \lesssim \delta \lesssim 30\,\mathrm{keV}$ are allowed. We note, however, that the precise width of these intervals is quite sensitive to small deviations in the constraint curves and in the signal. A combination of constraints from all null experiments is critical in obtaining this picture; XENON and CDMSII-Ge constraints are most important for positive δ, while CRESST and CDMSII-Si close off the negative δ window. The largest range of allowed dark matter masses occurs for $\delta \approx 0$, indicating that inelastic scattering processes are not very helpful in reconciling the DAMA signal with other experimental constraints.

4. Conclusions

We have studied the consistency of the dark matter interpretation of the annual modulation signal observed by DAMA with the results of the null experiments CDMS, CRESST, and XENON. Recent work has shown the presence of a channeling effect in the crystal scintillators utilized by DAMA which drastically changes the interpretation of the experimental results. The presence of the channeling effect opens a window in dark matter parameter space between 3 and 8 GeV where the DAMA signal is consistent with all of the null experiments. This consistency requires no exotic dark matter physics — a vanilla,
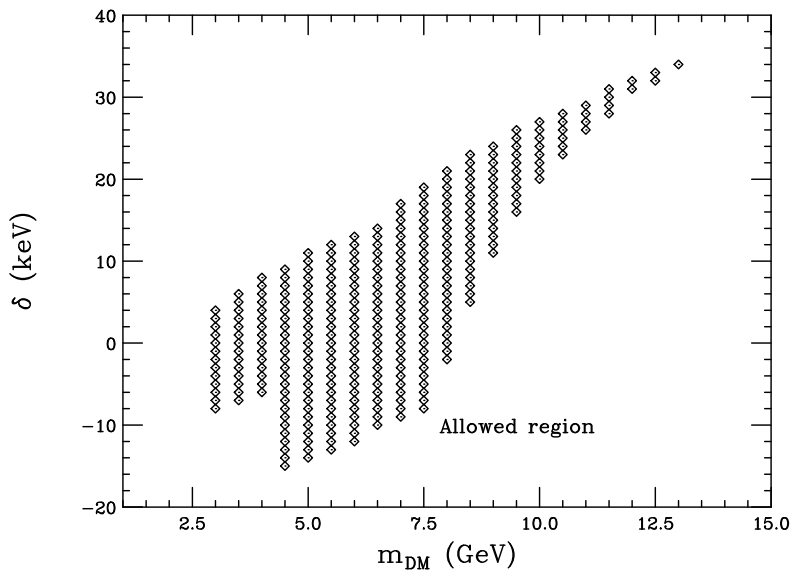
Figure 7: Region of parameter space in the $m_{\rm DM}, \delta$ plane where the DAMA signal is consistent with the constraints from all null experiments. The widest allowed range of dark matter masses occurs where $\delta = 0$.

elastically scattering dark matter candidate interacting through spin-independent channels is sufficient to explain both the signal and the null results from the other experiments. We have also examined whether possible inelastic processes can accommodate all experimental results. Inelastic scattering of dark matter particles to heavier final states renders dark matter masses up to approximately $13\,{\rm GeV}$ consistent with all measurements. However, the largest range of permissible dark matter masses occurs for elastic scattering candidates, indicating that inelastic processes do not open up significant regions of parameter space. Future measurements from ultra-low energy germanium detectors and silicon results from CDMS are needed to explore this light-mass window.

The light dark matter window suggested by the DAMA results motivates many new directions for model-building and phenomenology with low-mass WIMP candidates. Although more model-dependent, the implications of light dark matter for indirect detection and collider experiments should be explored. It would be interesting to also consider whether spin-dependent scattering allows a larger range of dark matter masses to be consistent with DAMA and the null experiments.

Acknowledgments

References

[1] DAMA collaboration, R. Bernabei et al., *First results from DAMA/LIBRA and the combined results with DAMA/NaI*, `arXiv:0804.2741`.

[2] CDMS collaboration, D.S. Akerib et al., *New results from the Cryogenic Dark Matter Search experiment*, *Phys. Rev.* **D 68** (2003) 082002 [`hep-ex/0306001`].

[3] CDMS collaboration, Z. Ahmed et al., *A search for WIMPs with the first five-tower data from CDMS*, `arXiv:0802.3530`.

[4] CDMS collaboration, D.S. Akerib et al., *Limits on spin-independent WIMP nucleon interactions from the two-tower run of the Cryogenic Dark Matter Search*, *Phys. Rev. Lett.* **96** (2006) 011302 [`astro-ph/0509259`].

[5] XENON collaboration, J. Angle et al., *First Results from the XENON10 dark matter experiment at the Gran Sasso National Laboratory*, *Phys. Rev. Lett.* **100** (2008) 021303 [`arXiv:0706.0039`].

[6] L.J. Hall, T. Moroi and H. Murayama, *Sneutrino cold dark matter with lepton-number violation*, *Phys. Lett.* **B 424** (1998) 305 [`hep-ph/9712515`].

[7] D. Tucker-Smith and N. Weiner, *Inelastic dark matter*, *Phys. Rev.* **D 64** (2001) 043502 [`hep-ph/0101138`].

[8] D. Tucker-Smith and N. Weiner, *The status of inelastic dark matter*, *Phys. Rev.* **D 72** (2005) 063509 [`hep-ph/0402065`].

[9] DAMA collaboration, R. Bernabei et al., *Investigation on light dark matter*, `arXiv:0802.4336`.

[10] R. Foot, *Implications of the DAMA/NaI and CDMS experiments for mirror matter-type dark matter*, *Phys. Rev.* **D 74** (2006) 023514 [`astro-ph/0510705`].

[11] R. Foot, *Mirror dark matter and the new DAMA/LIBRA results: a simple explanation for a beautiful experiment*, *Phys. Rev.* **D 78** (2008) 043529 [`arXiv:0804.4518`].

[12] M.Y. Khlopov, *Composite dark matter from stable charged constituents*, `arXiv:0806.3581`.

[13] G. Gelmini and P. Gondolo, *DAMA dark matter detection compatible with other searches*, `hep-ph/0405278`.

[14] P. Gondolo and G. Gelmini, *ComPatibility of DAMA dark matter detection with other searches*, *Phys. Rev.* **D 71** (2005) 123520 [`hep-ph/0504010`].

[15] P. Ullio, M. Kamionkowski and P. Vogel, *Spin dependent WIMPs in DAMA?*, *JHEP* **07** (2001) 044 [`hep-ph/0010036`];
A. Kurylov and M. Kamionkowski, *Generalized analysis of weakly-interacting massive particle searches*, *Phys. Rev.* **D 69** (2004) 063503 [`hep-ph/0307185`].

[16] E.M. Drobyshevski, *Channeling effect and improvement of the efficiency of charged particle registration with crystal scintillators*, `arXiv:0706.3095`.

[17] R. Bernabei et al., *Possible implications of the channeling effect in NaI(Tl) crystals*, *Eur. Phys. J.* **C 53** (2008) 205 [`arXiv:0710.0288`].

[18] For some discussion of these issues, see E. Newman and F.E. Steigert, *Response of NaI(Tl) to energetic heavy ions*, *Phys. Rev.* **118** (1960) 1575;
M. Luntz and R.H. Bartram *Stopping power and luminescent-response calculation for channeling in NaI(Tl) and CsI(Tl)*, *Phys. Rev.* **175** (1968) 468;
M.R. Altman et al., *Scintillation response of NaI(T1) and KI(T1) to channeled ions*, *Phys. Rev.* **B 7** (1973) 1743;
R.W. Birkmire, R.B. Murray and M. Luntz, *Scintillation response of nonactivated and activated NaI to random and channeled ions: influence of the luminescence mechanism*, *Phys. Rev.* **B 15** (1977) 31;
J. Graichen et al., *Efficiency and directional effects in the detection of low-energy recoil nuclei in a NaI(Tl) single crystal.*, *Nucl. Instrum. Meth.* **A485** (2002) 774 [*Erratum ibid.* **501** (2003) 630].

[19] C.E. Aalseth et al., *Experimental constraints on a dark matter origin for the DAMA annual modulation effect*, arXiv:0807.0879.

[20] G. Angloher et al. *Limits on WIMP dark matter using sapphire cryogenic detectors*, *Astropart. Phys.* **18** (2002) 43.

[21] P.S. Barbeau, J.I. Collar and O. Tench, *Large-mass ultra-low noise Germanium detectors: performance and applications in neutrino and astroparticle physics*, *JCAP* **09** (2007) 009 [nucl-ex/0701012].

[22] TEXONO collaboration, S.T. Lin et al., *New limits on spin-independent couplings of low-mass WIMP dark matter with a germanium detector at a threshold of* 200 eV, arXiv:0712.1645.

[23] I. Avignone, F. T., P.S. Barbeau and J.I. Collar, *Comments on new limits on spin-independent couplings of low-mass WIMP dark matter with a Germanium detector at a threshold of* 200 eV, arXiv:0806.1341.

[24] J.F. Gunion, D. Hooper and B. McElrath, *Light neutralino dark matter in the NMSSM*, *Phys. Rev.* **D 73** (2006) 015011 [hep-ph/0509024].

[25] V. Barger, P. Langacker and H.-S. Lee, *Lightest neutralino in extensions of the MSSM*, *Phys. Lett.* **B 630** (2005) 85 [hep-ph/0508027].

[26] D. Hooper and K.M. Zurek, *A natural supersymmetric model with MeV dark matter*, *Phys. Rev.* **D 77** (2008) 087302 [arXiv:0801.3686].

[27] J.L. Feng and J. Kumar, *The WIMPless miracle*, arXiv:0803.4196.

[28] J.L. Feng, J. Kumar and L.E. Strigari, *Explaining the DAMA signal with WIMPless dark matter*, arXiv:0806.3746.

[29] A. Bottino, N. Fornengo and S. Scopel, *Light relic neutralinos*, *Phys. Rev.* **D 67** (2003) 063519 [hep-ph/0212379];
A. Bottino, F. Donato, N. Fornengo and S. Scopel, *Lower bound on the neutralino mass from new data on CMB and implications for relic neutralinos*, *Phys. Rev.* **D 68** (2003) 043506 [hep-ph/0304080]; *Light neutralinos and WIMP direct searches*, *Phys. Rev.* **D 69** (2004) 037302 [hep-ph/0307303].

[30] A. Bottino, F. Donato, N. Fornengo and S. Scopel, *Zooming in on light relic neutralinos by direct detection and measurements of galactic antimatter*, *Phys. Rev.* **D 77** (2008) 015002 [arXiv:0710.0553].

[31] D.B. Kaplan, *A Single explanation for both the baryon and dark matter densities*, *Phys. Rev. Lett.* **68** (1992) 741;
S.M. Barr, *Baryogenesis, sphalerons and the cogeneration of dark matter*, *Phys. Rev.* **D 44** (1991) 3062.

[32] G.R. Farrar and G. Zaharijas, *Dark matter and the baryon asymmetry*, *Phys. Rev. Lett.* **96** (2006) 041302 [`hep-ph/0510079`].

[33] R. Kitano and I. Low, *Dark matter from baryon asymmetry*, *Phys. Rev.* **D 71** (2005) 023510 [`hep-ph/0411133`].

[34] D.E. Kaplan, M. Luty and K. Zurek, work in progress.

[35] C.S. Kochanek, *The mass of the Milky Way galaxy*, *Astrophys. J.* **457** (1996) 228 [`astro-ph/9505068`].

[36] G. Jungman, M. Kamionkowski and K. Griest, *Supersymmetric dark matter*, *Phys. Rept.* **267** (1996) 195 [`hep-ph/9506380`].

[37] R.H. Helm, *Inelastic and elastic scattering of* 187 *MeV electrons from selected even-even nuclei*, *Phys. Rev.* **104** (1956) 1466.

[38] S. Yellin, *Finding an upper limit in the presence of unknown background*, *Phys. Rev.* **D 66** (2002) 032005 [`physics/0203002`].

[39] J. Filippini and R. Gaitskell, *Direct detection of WIMP dark matter, sensitivity plots*, http://dendera.berkeley.edu/plotter/entryform.html.